European Journal of Human Genetics (2008) 16, 1176–1186

www.nature.com/ejhg

ARTICLE

A missense mutation in *ALDH18A1*, encoding Δ^1-pyrroline-5-carboxylate synthase (P5CS), causes an autosomal recessive neurocutaneous syndrome

Louise S Bicknell[1], James Pitt[2], Salim Aftimos[3], Ram Ramadas[4], Marion A Maw[5] and Stephen P Robertson*[,1]

[1]*Department of Paediatrics and Child Health, University of Otago, Dunedin, New Zealand;* [2]*Genetic Health Services Victoria, Murdoch Children's Research Institute, Royal Children's Hospital, Melbourne, Australia;* [3]*Northern Regional Genetic Services, Auckland Hospital, Auckland, New Zealand;* [4]*Whakatane Hospital, Whakatane, New Zealand;* [5]*Department of Biochemistry, University of Otago, Dunedin, New Zealand*

There are several rare syndromes combining wrinkled, redundant skin and neurological abnormalities. Although phenotypic overlap between conditions has suggested that some might be allelic to one another, the aetiology for many of them remains unknown. A consanguineous New Zealand Maori family has been characterised that segregates an autosomal recessive connective tissue disorder (joint dislocations, lax skin) associated with neurological abnormalities (severe global developmental delay, choreoathetosis) without metabolic abnormalities in four affected children. A genome-screen performed under a hypothesis of homozygosity by descent for an ancestral mutation, identified a locus at 10q23 ($Z = 3.63$). One gene within the candidate interval, *ALDH18A1*, encoding Δ^1-pyrroline-5-carboxylate synthase (P5CS), was considered a plausible disease gene since a missense mutation had previously been shown to cause progressive neurodegeneration, cataracts, skin laxity, joint dislocations and metabolic derangement in a consanguineous Algerian family. A missense mutation, 2350C > T, was identified in *ALDH18A1*, which predicts the substitution H784Y. H784 is invariant across all phyla and lies within a previously unrecognised, conserved C-terminal motif in P5CS. In an *in vivo* assay of flux through this metabolic pathway using dermal fibroblasts obtained from an affected individual, proline and ornithine biosynthetic activity of P5CS was not affected by the H784Y substitution. These data suggest that P5CS may possess additional uncharacterised functions that affect connective tissue and central nervous system function.
European Journal of Human Genetics (2008) **16,** 1176–1186; doi:10.1038/ejhg.2008.91; published online 14 May 2008

Keywords: *ALDH18A1*; P5CS; proline; neurocutaneous

Introduction

There are several characterised disorders that manifest wrinkled, lax skin as a cardinal clinical sign and are often associated with impaired neurodevelopment. Such conditions include cutis laxa (OMIM 219200), wrinkly skin syndrome (OMIM 278250), and de Barsy syndrome (OMIM 219150). Cutis laxa is a genetically heterogeneous disorder characterised by loose and redundant skin.[1] There are three different categories based on the mode of inheritance. In the autosomal dominant group (OMIM 123700) skin laxity is late in onset and the disorder is caused by mutations in the elastin gene, *ELN*.[2] The X-linked recessive variety, also called occipital horn syndrome (OMIM 304150), is due to

*Correspondence: Professor S Robertson, Department of Paediatrics and Child Health, Dunedin School of Medicine, University of Otago, PO Box 913, Dunedin 9001, New Zealand.
Tel: 64 3 479 7469; Fax: 64 3 479 7469;
E-mail: stephen.robertson@stonebow.otago.ac.nz
Received 18 December 2007; revised 26 March 2008; accepted 3 April 2008; published online 14 May 2008

mutations in the copper transporting ATPase, *ATP7A*.[3] The third category is defined by an autosomal recessive mode of inheritance and composes two types. Type I (OMIM 219100) is associated with early pulmonary emphysema, a poor prognosis, and missense mutations in *FBLN4* and *FBLN5*.[4,5] Type II (cutis laxa with growth and developmental delay, CLGDD; OMIM 219200) is characterised by growth and developmental delay, joint laxity, characteristic facies and large fontanelles.[6] Abnormal glycan biosynthesis, in the absence of secondary defects of glycosylation, was recently identified in two cohorts of CLGDD patients,[7,8] and subsequently mutations in either the vesicular H^+-ATPase subunit gene *ATP6V0A2*, or the conserved oligomeric Golgi complex gene *COG7* have been identified.[9,10] Whether CLGDD and wrinkly skin syndrome represent separate entities or are variations of the same condition is controversial.[1,11–16] Wrinkly skin syndrome presents with less marked facial dysmorphism, than CLGDD, has milder cutaneous manifestations[1] and subtle differences in the elastic fibre derangement.[13] Significantly, however, the descriptions of both conditions originated from two independent reports of the same two siblings, complicating differential diagnosis.[16–18] De Barsy syndrome is an autosomal recessive syndrome in which corneal clouding is a near ubiquitous and defining phenotypic feature, that facilitates diagnosis.[19–21]

A new neurocutaneous disorder has recently been described in a consanguineous Algerian family with two affected sibs presenting with an inborn error of metabolism suggestive of a urea cycle defect (hypoprolinaemia, hypoornithinaemia, hypocitrullinaemia, hypoarginaemia and hyperammonaemia). The connective abnormalities included joint laxity and skin hyperelasticity in conjunction with mental retardation. The metabolic abnormalities observed in the affected individuals suggested *ALDH18A1* (OMIM 138250), encoding Δ^1-pyrroline-5-carboxylate synthase (P5CS) (EC 1.2.1.41, 2.7.2.11), as a candidate gene and subsequently both affected sibs were shown to be homozygous for a missense mutation (251G > A), predicting the amino acid substitution R84Q.[22,23] *In vitro* experiments established that the R84Q substitution lead to reduced steady state levels of P5CS protein with consequent impairment of proline and ornithine biosynthesis.[22,23] P5CS metabolises glutamate in the first step of proline and ornithine biosynthesis, prior to incorporation of ornithine in the urea cycle. The N-terminal γ-glutamyl kinase domain of P5CS catalyses the conversion of glutamate to γ-glutamyl phosphate in an ATP-dependent manner, which is then converted to glutamate γ-semialdehyde with concomitant NADPH reduction by the second major domain in P5CS, the γ-glutamyl phosphate reductase domain. Glutamate γ-semialdehyde is then spontaneously converted to Δ^1-pyrroline-5-carboxylate (P5C), the common intermediate in both proline and ornithine biosynthesis. P5C can be converted to proline by P5C reductase, or metabolised to ornithine by ornithine aminotransferase (Figure 1). The demonstration that conversion of glutamate to glutamate γ-semialdehyde occurs in the mitochondrion, and the presence of a mitochondrial targeting motif at the N terminus of P5CS suggested that P5CS localises to this organelle,[24,25] although direct evidence to exclude localisation to other cellular compartments is lacking.

In this report a recessive neurocutaneous syndrome segregating in a consanguineous New Zealand family is shown to be associated with a substitution of a phylogenetically invariant residue in P5CS. The measurement of metabolic flux through pathways relating to the established function of P5CS in patient fibroblasts using isotopically labelled substrate found that the H784Y substitution did not impair proline biosynthesis. These data suggest that this neuroconnective tissue phenotype may have arisen through the disruption of an unappreciated function of P5CS.

Materials and methods

Participation of subjects in this study took place after all individuals or their legal guardians gave full informed consent as approved by the Otago Ethics Committee.

Genetic mapping and linkage analysis

DNA samples from 11 family members were genotyped using the LMSV2 382 Marker Set, comprising 382 microsatellite markers spaced, on average, 10 cM apart across the genome (Australian Genome Research Facility, Melbourne, Australia). For fine mapping of microsatellites, primer sequences were obtained from UniSTS (http://www.ncbi.nlm.nih.gov/entrez/query.fcgi?db = unists), and labelled with ^{33}P α-ATP (Amersham, Bucks, UK) during PCR

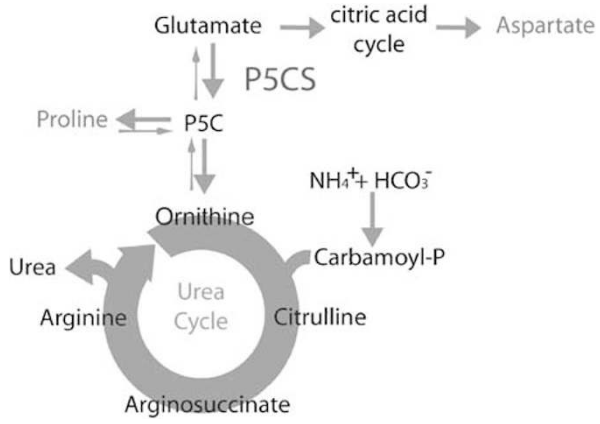

Figure 1 Proline and ornithine biosynthesis from glutamate. Δ^1-pyrroline-5-carboxylate synthase (P5CS) catalyses the conversion of glutamate to γ-glutamate semialdehyde, which is in non-enzymatic equilibrium with Δ^1-pyrroline-5-carboxylate (P5C). P5C reductase then metabolises P5C to proline. Ornithine aminotransferase catalyses the conversion of P5C to ornithine, which is then incorporated into the urea cycle.

amplification. PCR amplification was performed using the GeneAmp buffer system and AmpliTaq Gold (Applied Biosystems, Foster City, CA, USA). Microsatellites were genotyped by polyacrylamide gel electrophoresis and exposure to radiographic film (Kodak Biomax XAR film). Linkage analysis was performed using MLINK from the FASTLINK package of software, and Genehunter2.[26,27] The parameters assigned to the syndrome for the purpose of the analysis were those of an autosomal recessive disorder with a disease allele frequency of 0.0001. The number of alleles for each microsatellite was calculated by combining genetic information from several New Zealand families with the minimum allele number set at five; all alleles were assumed to have equal frequency in the population. Genetic locations of the genotyped microsatellites were taken from the Généthon genetic map[28] or inferred from flanking microsatellite markers.

Candidate gene screening

All exons and exon/intron boundaries of *ALDH18A1* were amplified using the GeneAmp buffer system and AmpliTaq Gold (Applied Biosystems; primer sequences and amplification conditions available on request). Amplicons were sequenced with ABI BigDye Terminator cycle sequencing v3.1 (Applied Biosystems) on an ABI 3700 Sequencer. Sequence results were analysed using Sequencher software (Gene Codes, Ann Arbor, Michigan, USA). A mismatched primer was designed to create an *Xmn* I restriction fragment length polymorphism that allows discrimination of the mutation and wildtype allele within exon 18 of *ALDH18A1* (sequences available on request). The C (wildtype) allele permits digestion of a 201 (bp) exon 18 fragment into 179 and 22 bp while the *Xmn* I site is abolished in the T (disease) allele. For screening of control chromosomes, Maori controls were assigned based on the ethnicity of the four grandparents. All Maori descendants have a mixture of European and Maori ancestry, and therefore it was appropriate to test control chromosomes from both European and Maori ethnic groups.

A cellular assay for P5CS activity

Cultured dermal fibroblast cells (3.3×10^5) from an affected male patient and a male control were seeded and incubated in Hanks Basic Salt Solution (HBSS) (Gibco) supplemented with 5 mM glucose, 1% penicillin/streptomycin and 2 mM either L-glutamic acid (Sigma) or $^{13}C_5$-glutamic acid (Cambridge Isotope Laboratories Inc., Massachusetts, USA) for 12 h in 5% CO_2 atmosphere at 37°C. Cells were harvested by trypsinisation, and protein denatured by absolute ethanol. Samples were hydrolysed *in vacuuo* at 160°C for 1 h using 6 M HCl and 0.1% (v/v) phenol. Amino acids were converted to *N*-propoxycarbonyl propyl esters derivatives[29] and analysed using liquid chromatography-mass spectrometry. Following hydrolysis, residues were reconstituted with 32 μl of pyridine:water (135:1018, v:v) containing 37 nmol of $^2H_8$-valine as an internal standard. Eighteen microlitres of n-propanol:propylchloroformate (155:15, v:v) was added with vortexing and the mixture incubated at room temperature for 5 min followed by addition of 200 μl of methanol:water:acetic acid (500:500:20 v:v:v) and mixing. A 2.1×100 mm 5 μm Hypersil ODS column with a 2.1×12.5 mm 5 μm Extend C18 guard column (Agilent) was used to separate the amino acid derivatives. Buffer A was 9:1 (v:v) water:0.2 M ammonium formate pH 3.5 while buffer B was 9:1 (v:v) methanol:0.2 ammonium formate pH 3.5 and a flow rate of 0.2 ml/min was used. After injection of 20 μl of derivatised amino acids the column was held at 50% buffer B for 1 min, after which a linear ramp to 100% buffer B at 5 min was applied and the column held at 100% buffer B until 8 min. The column was connected to a Quattro LC electrospray tandem mass spectrometer (Waters Corporation) operating in single MS positive ion mode with recording of 254, 244, 249, 304, 308, 318 and 323 *m/z* for $^2H_8$-valine, proline, $^{13}C_5$-proline, aspartate, $^{13}C_4$-aspartate, glutamate and $^{13}C_5$-glutamate respectively.

Immunocytochemistry

Patient and control fibroblasts were cultured in DMEM supplemented with 10% (v/v) fetal calf serum, 2 mM L-glutamine and 100 U each of penicillin and streptomycin in a 5% CO_2 atmosphere at 37°C. Cells (1.5×10^4) were seeded onto 10 mm round coverslips, and incubated in media containing 250 nM Mitotracker CMXRos (Molecular Probes) for 1 h at 37°C. Cells were washed two times with PBS and then fixed in 1% (w/v) paraformaldehyde for 2 min. Cells were washed, then permeabilised and blocked in 5% (w/v) bovine serum albumin, 2% (w/v) goat serum and 0.2% (v/v) Triton X-100, for 1 h at room temperature. Following brief washing, cells were incubated with mouse polyclonal α-human α-P5CS antibody (Abnova Corp, Taiwan), at room temperature for 2 h. Cells were washed, and then α-P5CS was detected by the incubation of goat α-mouse Alexa Fluor 488 (Molecular Probes) for 1 h at room temperature. The nucleus was visualised by staining with diluted DAPI for 3 min. Coverslips were mounted in Glycergel (Dako), and images were captured using a Zeiss LSM 510 axioplan2 confocal microscope.

Results

Clinical presentation

A New Zealand Maori family was ascertained that segregated a neurocutaneous syndrome that did not unequivocally fit any previously described disorder. The parents are first cousins and have 10 children, four of whom are affected (Figure 2). All children were born at term after unremarkable pregnancies. There were no exposures to drugs or other teratogens, Apgar scores were normal in all instances and birth weights ranged between 1.8–3.1 kg. All

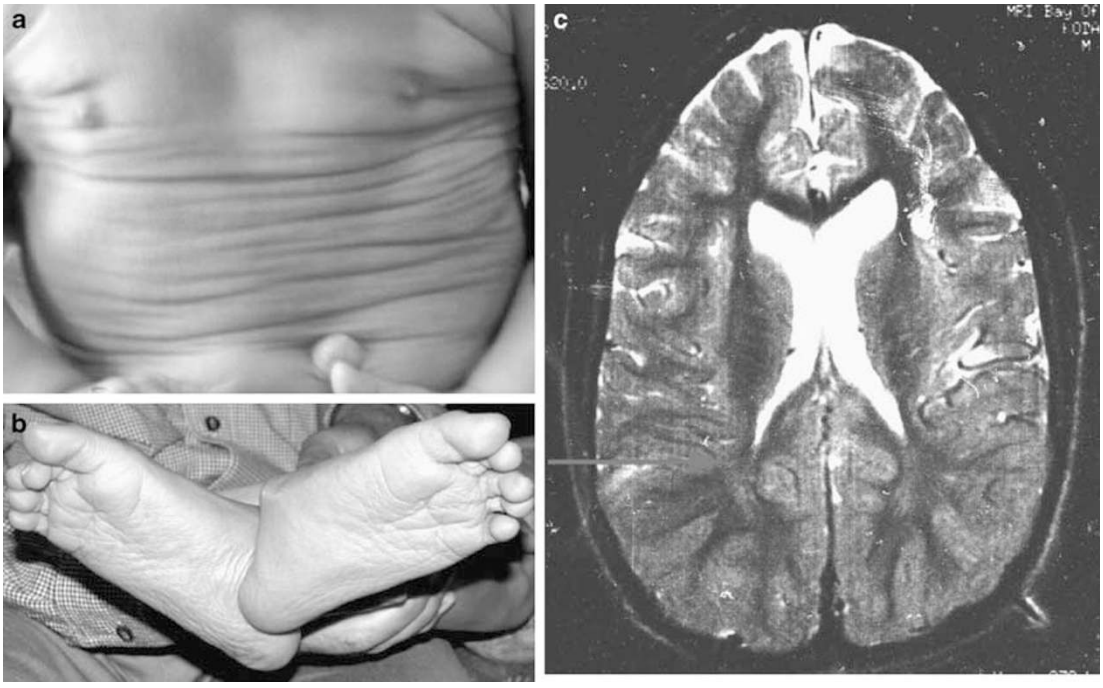

Figure 2 Phenotype features of the new neurocutaneous disorder segregating in a consanguineous family. Lax skin is shown in (**a**) abdomen of a 6-month-old baby and (**b**) soles of feet of a 9-year-old child. (**c**) T_2 axial MRI brain scan of individual IV-4 demonstrating marked underdevelopment of the white matter particularly in the peritrigonal region of the cerebral cortex. Regions of the insular cortex nearly abut the margins of the ventricles (red arrow).

affected sibs had head circumferences below the second centile at birth (Table 1). At time of assessment, the affected children were aged 22, 12, 11 and 4 years, respectively. Detailed phenotypic information is presented in Table 1. The four affected individuals show pronounced abnormalities of connective tissue. Most notably, the skin over hands, feet, abdomen, chest and face was very wrinkled (Figure 2). The skin, although lax, was not hyperelastic; wounds healed normally and the skin did not scar excessively. There was neither a predisposition to bruising nor a bleeding diathesis. With age the wrinkliness of the skin disappeared so that by adolescence it was no longer clinically evident. Two of the four probands had bilateral dislocation of the hips at birth and both required operative intervention. One child required repeated surgery with recurrent failure to relocate the hips bilaterally by age 5 years. A third child (IV-4) developed bilateral dislocation of the hips at age 12 years, unrelated to any identifiable instance of trauma. During early childhood hypermobility of the elbows, wrists, small joints of the hands and knees was a constant clinical feature. With advancing age this became less obvious, especially with co-evolution of hypertonicity in the lower limbs.

The children had mild proportionate short stature (lengths between −3 and −2 SD). One individual had a kyphoscoliosis. A skeletal survey was performed on IV-4 at 8 years and was normal except for delayed ossification of the distal femoral epiphysis and multiple growth arrest lines within the metaphyses of the long bones.

Global neurodevelopmental delay was evident from early infancy and presented as a static encephalopathy. Seizures were noted in two individuals from day 2 of life but remitted by the end of the first week and have never recurred. Congenital microcephaly was noted in all and has persisted but has not progressed. An MRI brain scan performed in one affected child (Figure 2) demonstrated a relative paucity of white matter especially in the region of the trigones but also notable in the frontal and temporal lobes, and thinning of the corpus callosum. Signal intensity of the white matter was within normal limits indicating normal myelination for age. Individual IV-4 had bilateral lamellar nuclear cataracts.

Biochemical investigations

There were no significant abnormalities from extensive biochemical investigations. Fasting and post-protein load amino acid profiles were also obtained in three affected individuals; IV-1 at 21 years, IV-4 at 11 years and IV-5 at 10 years. Table 2 lists the relevant serum biochemistry from affected children in both fasting and fed states. All amino acids levels were within the normal range apart from mild post-prandial hypoornithinaemia in individuals IV-4 and IV-5.

Table 1 Phenotypic features of four affected individuals in the New Zealand family

	Phenotypic feature	*Individual IV-1*	*Individual IV-4*	*Individual IV-5*	*Individual IV-9*	*Proportion*
Postnatal	Birth weight	<1.8 kg	2.4 kg	2.3 kg	3.1 kg	4/4
	Hypotonia	+	+	+	+	4/4
	Failure to thrive	+	+	+	+	4/4
Connective tissue	Short stature	−2SD	−3SD	−2SD	NA	3/3
	Scoliosis	−	+	−	−	1/4
	Hip dislocation	−	Bilateral occurred at 12 years	Bilateral congenital	Bilateral congenital	3/4
	Inguinal hernia	−	Right	−	−	1/4
	Lax Skin					
	Hands	+	+	+	+	4/4
	Feet	+	+	+	+	4/4
	Abdomen/ chest	−	+	+	+	3/4
	Visible veins	Thorax and abdomen	Thorax and abdomen	Thorax and abdomen	Thorax and abdomen	4/4
	Cataract	−	+	−	−	1/4
Development	*Limb tone*					
	Upper	Normal	+	Normal	Increased	2/4
	Lower	Increased	Increased	Increased	Increased	4/4
	Muscle bulk	Distal wasting	Distal wasting	Distal wasting	Distal wasting	4/4
	Reflexes	Brisk (downgoing plantars)	Brisk (downgoing plantars)	Brisk	Brisk particularly in lower limbs	4/4
	Walking	Standing frame	Unable	Standing frame	Unable	2/4
	Athetosis	+	−	+	−	2/4
	Speech	Absent	Absent	Absent	Absent	4/4
	Developmental delay	Severe	Severe	Severe	Severe	4/4
	Head circumference	<2nd centile	<2nd centile	<2nd centile	<2nd centile	4/4

Table 2 Serum biochemistry of affected individuals

	IV-1		*IV-4*		*IV-5*		*Lab reference range*
	Fasting	*Fed*	*Fasting*	*Fed*	*Fasting*	*Fed*	
Glutamate	16	25	19	28	22	50	12–104
Proline	197	264	122	374	120	167	59–369
Ornithine	34	47	24[a]	39	20[a]	35	27–107
Citrulline	12	18	13	23	10	19	10–47
Arginine	54	96	52	79	56	91	36–124
Ammonia	23	23	NA	NA	22	33	0–70

NA, not available.
All values in μmol/l.
[a]Levels are outside of the reference range.

Differential diagnosis

The phenotype studied here is not typical for any previously described neurocutaneous syndrome. On the basis of the connective tissue defects (lax skin and joints), it has the most similarity to de Barsy syndrome than any other lax skin syndrome (Table 3). However, a characteristic feature in de Barsy syndrome, that of corneal clouding, is absent in this family, making the assignment of this diagnosis inappropriate.

Identification of a mutation in *ALDH18A1*

The rarity of this phenotype in combination with consanguinity in a family with four affected individuals made mapping the disease gene for this condition under a linkage hypothesis of homozygosity by descent a plausible approach. A 382-microsatellite whole genome screen was performed. Following two point linkage analysis, loci demonstrating LOD scores of $Z>1.5$ (at 4p15.3, 10p13 and 10q24), were fine-mapped. Multipoint analysis demonstrated that 77.9% of the genome could be excluded from linkage at a statistically significant threshold ($Z<-2$), while 96.2% of the genome demonstrated an LOD score of $Z<0$. Following fine mapping the only locus with a significant LOD score ($Z>3.3$) using Genehunter2 was at 10q23.1–10q24.1 ($Z=3.63$). A 19 cM critical region delimited by microsatellites *D10S1686* and *D10S1758* was defined based on segregation of a common ancestral haplotype, a finding congruent with the linkage hypothesis (Figure 3). This critical region corresponded to a physical region of 14 Mb within which there were 112 annotated and unannotated genes to be considered for candidacy as the disease gene (Ensembl Genome Build 26, Nov 2004).

The previous description of a consanguineous Algerian family segregating a similar phenotype to the family under study associated with a missense mutation in *ALDH18A1*, presented this gene as the prime disease gene candidate. A missense mutation, 2350C>T, was identified in exon 18 of *ALDH18A1*, and predicts the amino acid substitution H784Y in the encoded protein P5CS (Figure 4). This

Table 3 Differential diagnosis of cutis laxa-mental retardation syndromes

Phenotypic features	*Cutis laxa type II*	*Wrinkly skin syndrome*	*de Barsy syndrome*	*New Zealand family*
Lax skin	+	+	+	+
Progeriod appearance	–	–	+	+
Joint dislocations	+	+	+	+
Winged scapulae	–	+	–	–
Spinal deformities/scoliosis	–	+	–	+ (1/4)
Large fontanelles	+	–	–	–
Microcephaly	–	+	+	+
Characteristic facies	+	–	–	–
Inguinal hernia	–	–	+	+ (1/4)
Intra-uterine growth retardation	+	+	–	+
Postnatal growth failure	+	+	–	+
Hypotonia	–	–	+	+
Developmental delay	+	+	+	+
Athetosis	–	–	+	+
White matter underdevelopment	–	–	–	+
Elastic fibre abnormalities	+	+	+	NA

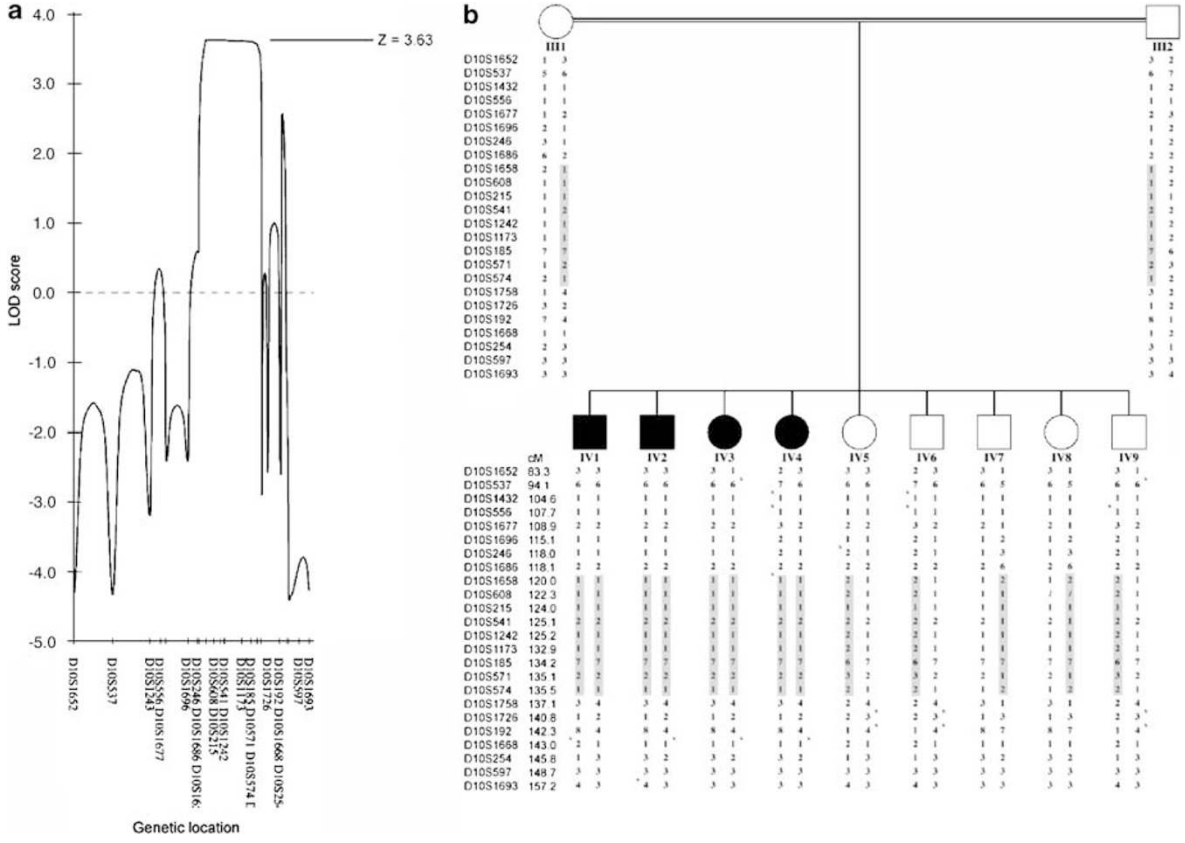

Figure 3 Multipoint linkage analysis and haplotype construction of 10q21.3–10q25.1 following fine-scale genotyping. (**a**) Multipoint linkage analysis using Genehunter2 gave a maximal LOD score of $Z = 3.63$ between microsatellites *D10S1686* and *D10S1758* following fine mapping in individuals from the New Zealand family. (**b**) Haplotype construction by Genehunter2. The boxes delineate the haplotype present in a homozygous manner exclusively in the affected individuals and present in only one copy in non-affected individuals. X marks positions of recombination events as determined by haplotype construction using Genehunter2. Genotypes in italics (IV-8, D10S608) were inferred by Genehunter2 after failure during genotyping.

sequence change is not reported as a polymorphism in dbSNP (http://www.ncbi.nlm.nih.gov/projects/SNP/). Restriction endonuclease digestion demonstrated only affected individuals who were homozygous for 2350T (Figure 4). The 2350C > T mutation was not found in samples obtained from healthy controls (726 European, 106 Maori and 56 Pacific

Islander chromosomes) using a restriction fragment length polymorphism assay. The absence of the 2350T allele in a population this size gives an estimated allele frequency of 0.0011 (95% confidence interval: 0, 0.00336).

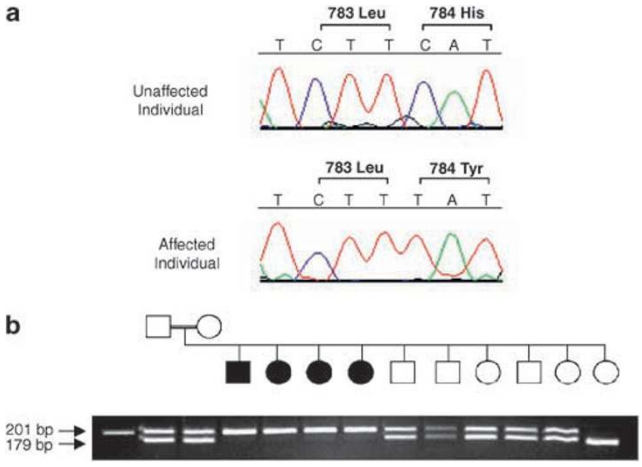

Figure 4 Identification of the missense mutation 2350C>T in *ALDH18A1*. (**a**) Chromatograms showing the mutation 2350C>T, predicted to lead to H784Y, in *ALDH18A1*. The mutations are homozygous in an affected individual and, absent in an unaffected control individual. (**b**) *Xmn* I digestion of PCR-amplified DNA from individuals in the entire family. A DNA ladder is present in lane 1 (200 base pairs), with the parents in lanes 2 and 3, the four affected offspring in lanes 4–7, and unaffected offspring in lanes 8–13. bp – base pairs.

H784 is completely conserved in orthologous proteins

To analyse the degree of conservation of H784, the sequences of P5CS orthologues from other species, including those of γ-glutamyl phosphate reductase proteins from organisms in which the two functional domains of mammalian P5CS are encoded by separate genes (prokaryotes, yeasts and fungi), were aligned using ClustalW (Figure 5). This analysis demonstrated that H784 is completely conserved within a previously unrecognised conserved motif in P5CS embedded in a C-terminal domain that is shared by all orthologous forms of this protein in eukaryotes. Analysis by SIFT[30] gave a score of 0.00 (where a score <0.05 predicts a deleterious substitution) indicating that the H784Y substitution would not be tolerated within this conserved domain.

H784Y does not impair proline biosynthesis from glutamate in patient fibroblasts

P5CS function in proline biosynthesis was studied in an *in vivo* assay using cultured primary dermal fibroblasts obtained from individual IV-4. Reduced flux through the glutamate-proline pathway, as measured by diminished production of proline normalised to control fibroblasts, would be indicative of deficiency of P5CS activity.

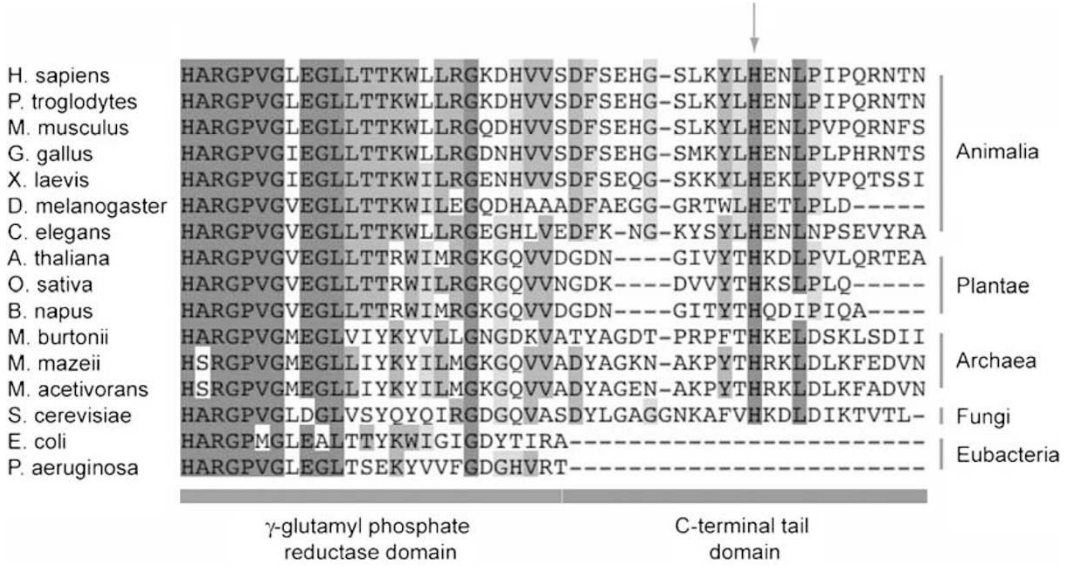

Figure 5 ClustalW alignment of P5CS or γ-glutamyl phosphate reductase amino acid sequences from different organisms. Shown is the C-terminal portion of the reductase domain and the C-terminal tail domain. Prokaryotes do not possess the C-terminal tail domain. The arrow indicates the position of H784. *H. sapiens – Homo sapiens* (RefSeq: NP_002851), *P. troglodytes – Pan troglodytes* (RefSeq: XM_001156006), *M. musculus – Mus musculus* (RefSeq: NM_019698), *G. gallus – Gallus gallus* (XP_421834), *X. laevis – Xenopus laevis* (RefSeq: NM_001092571), *D. melanogaster – Drosophila melanogaster* (RefSeq: NM_141118), *C. elegans – Caenorhabditis elegans* (RefSeq: NM_077731), *A. thaliana – Arabidopsis thaliana* (RefSeq: NM_115419), *O. sativa – Oryza sativa* (RefSeq: NM_001062258), *B. napus – Brassica napus* (AF314811), *M. burtonii – Methanococcoides burtonii* (RefSeq: NC_007955), *M. mazei – Methanosarcina mazei* (RefSeq: NC_003901), *M. acetivorans – Methanosarcina acetivorans* (RefSeq: NC_003552), *S. cerevisiae – Saccharomyces cerevisiae* (RefSeq: NC_001147), *E. coli – Escherichia coli* (RefSeq: NC_002655), *P. aeruginosa – Pseudomonas aeruginosa* (RefSeq: NC_002516.2).

Glutamate is also converted to aspartate via the citric acid cycle and flux through this independent pathway was used to normalise activity between and within patient and control cells. In four replicate experiments, fibroblasts were incubated with $^{13}C_5$-glutamate for 12 h, followed by cellular lysis, amino acid hydrolysis and determination of $^{13}C_5$-glutamate-derivatives by mass spectrometry.

Flux through the glutamate–aspartate pathway (measured by $^{13}C_4$-aspartate production) was similar in both patient and control cells in all replicate experiments ($P=0.73$, Students *t*-test), excluding a generalised deficiency in cellular activity or metabolism of glutamate to other amino acids in patient fibroblasts (Figure 6).

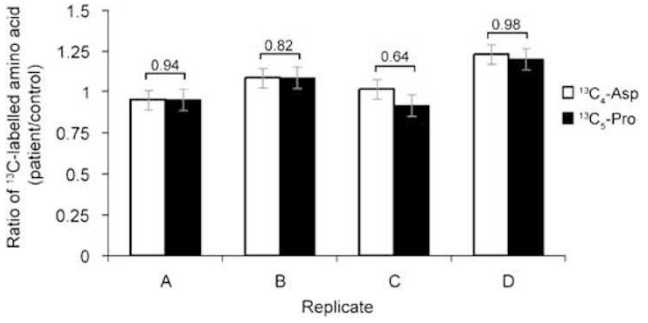

Figure 6 $^{13}C_5$-glutamic acid metabolism in primary human fibroblasts. Ratios of $^{13}C_4$-aspartate and $^{13}C_5$-proline in patient fibroblasts normalised to control fibroblasts in four replicate experiments. Error bars represent the SE from each experiment. Above each experiment are the *P*-values calculated using Student's *t*-test comparing the levels of $^{13}C_5$-proline and $^{13}C_4$-aspartate produced in patient *versus* control fibroblasts.

Proline biosynthesis (the ratio of $^{13}C_5$-proline to $^{13}C_5$-glutamate, normalised against control fibroblast proline biosynthesis) was not significantly different between patient and control cells ($P=0.86$, Student's *t*-test), indicating that flux in the glutamate–proline pathway was not diminished in patient cells in each of four replicate experiments (Figure 6). These data demonstrate that in this assay there was no deficiency in P5CS-mediated conversion of glutamate to proline in fibroblasts expressing P5CS with the H784Y substitution.

Immunocytochemistry

The cellular localisation of P5CS was determined in both patient and control fibroblasts by performing dual label confocal imaging with a mitochondrial-specific fluorescent marker Mitotracker CMXRos, and a polyclonal antibody raised against the C terminus of P5CS (Figure 7). These data demonstrated localisation of P5CS to a subpopulation of mitochondria in both patient and control fibroblasts. This confirms the previously suggested localisation of P5CS to within the mitochondrion, and indicates the H784Y substitution is not associated with large-scale aggregation or anomalous subcellular targeting of P5CS to another cellular compartment.

Discussion

Improving the understanding of the aetiology underlying the group of conditions that combine connective tissue dysfunction and neurological abnormalities would greatly improve genetic counselling for such individuals. In this

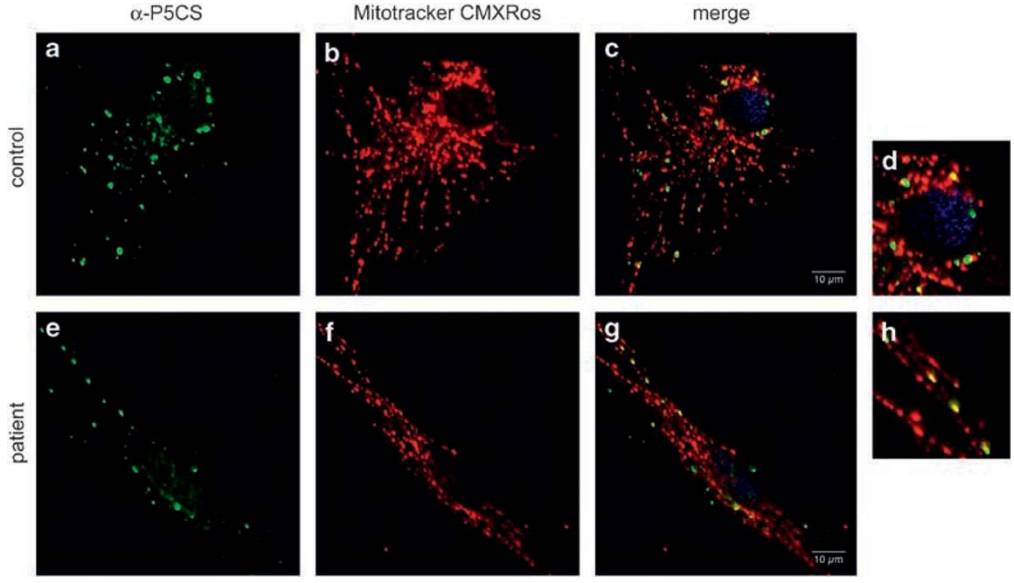

Figure 7 Cellular localisation of P5CS. Confocal immunocytochemistry of P5CS in control (**a**–**d**) and patient (**e**–**h**) dermal fibroblasts, staining for P5CS (**a**, **e**), mitochondria (**b**, **f**) and merged images with DAPI (**c**, **g**). (**d**, **h**) Magnified sections of merged images in **c** and **g**.

report a gene, *ALDH18A1*, previously associated with a phenotype combining neurocutaneous abnormalities and metabolic derangement, is studied in an unrelated family with a partially overlapping clinical presentation. These findings imply that the primary enzymatic functions of P5CS, the product of *ALDH18A1*, may not entirely account for all elements of these reported phenotypes.

A genome-wide linkage approach under an assumption of homozygosity by descent identified a 19 cM critical region at 10q23, and of the 112 genes to consider as candidate disease genes, *ALDH18A1* was prioritised based on its previous disease association and the function of the encoded protein in proline biosynthesis, a critical amino acid in collagen fibres in connective tissue. Despite the LOD score on multipoint analysis ($Z = 3.63$) exceeding the maximum threshold for genome-wide significance[31,32] it still remains a formal possibility that the linkage with *ALDH18A1*, is a false positive or that two separate conditions are segregating in this consanguineous family. Sequencing of *ALDH18A1* identified homozygosity for the missense mutation 2350C>T, predicting H784Y, in all affected individuals. Although it is possible that this sequence change is functionally neutral and that the true disease gene has not been identified there are strong grounds to consider 2350C>T in *ALDH18A1* as causative of the phenotype described here.

Firstly, restriction endonuclease digestion confirmed homozygosity for 2350T exclusively in affected individuals, as predicted by the linkage hypothesis of homozygosity by descent. The mutation was absent in a total of 888 chromosomes from healthy individuals, including 162 chromosomes that were ethnically matched. Additionally, this sequence change has not previously been identified as a polymorphism on public databases. Secondly, H784 is completely conserved throughout evolution in all phyla from mammals to fungi and yeast within a domain that showed significant levels of sequence conservation (Figure 5). On a cautionary note however, although SIFT analysis predicted this substitution to be deleterious, the overall higher degree of conservation in mitochondrial proteins as a whole does reduce the level of confidence underlying conclusions made by this methodology alone. Thirdly, one family has been previously reported with a genetic condition with phenotypic overlap to the entity described here and was associated with deficient P5CS function. Baumgartner *et al*[22], described a first cousin consanguineous Algerian family with two affected sibs who presented with a congenital metabolic and connective tissue disorder with progressive neurodevelopmental decline. The affected sibs were shown to be homozygous for a missense mutation (251G>A) in *ALDH18A1*. This predicts the substitution R84Q in the γ-glutamyl kinase domain in P5CS, which correlates with the demonstrated enzymatic deficiency. Importantly, this gene was screened on the basis of its established biochemical function, and not on positional linkage grounds as was the case in the family described in this report. Identification of a mutation in the same gene causing a similar phenotype, where the gene was identified through a genetic mapping strategy, strengthens evidence for this phenotype being caused by the mutation in *ALDH18A1*.

An *in vivo* enzymatic assay measuring flux through the glutamate-proline biosynthetic pathway demonstrated that the presence of the H784Y substitution in P5CS in fibroblasts derived from an affected individual showed no impairment of proline biosynthesis. A similar assay using tritium-labelled substrate demonstrated reduced flux through this pathway in fibroblast cells derived from affected sibs in the Algerian family with the R84Q substitution, complementing previous observations of reduced enzymatic activity in an *in vitro* assay of P5CS activity in a cell lysate.[22,23] The demonstration that a similar assay detected reduced flux through this pathway in the Algerian family supports its utility in studying the significance of the H784Y substitution associated with the phenotype described here. Furthermore, considering the mitochondrial localisation of P5CS, the use of an *in vivo* assay rather than more direct measures of *in vitro* enzymatic activity may replicate the cellular physiology more accurately.

The putative cellular localisation of P5CS to the mitochondrion was confirmed by immunocytochemistry in this study, with the added observation that there was no difference in localisation of this protein between patient and control fibroblasts (Figure 7). Furthermore, fluorescent detection of P5CS demonstrated that the H784Y substitution does not cause large-scale abnormal protein aggregation or mislocalisation within the cell.

A functional assay measuring proline biosynthesis led to the conclusion that the phenotype studied here is not attributable to deficiency of the established enzymatic function of P5CS. This is congruent with the metabolic indices measured in the affected sibs in this report but is in contrast to the sibs reported in the literature with the R84Q substitution who exhibited hypoprolinaemia, hypoornithinaemia, hypocitrullinaemia, hypoarginaemia and hyperammonaemia. Other aspects of the phenotype also differ suggesting some non-equivalence in the aetiopathogenesis of the phenotypes despite them likely being allelic to one another. For example, the Algerian sibs exhibited saltatory neurodevelopmental decline, possibly on account of recurrent episodes of hyperammonaemia. This observation is in contrast to the static developmental delay seen in affected children from the New Zealand family.

Further evidence consistent with the pathogenic effect of the H784Y substitution being independent of the proline biosynthetic function of P5CS is the observation that prokaryotes do not possess the C-terminal domain within which H784 is located, despite the known enzymatic function of these orthologous enzymes being conserved across all kingdoms. Therefore, the C-terminal tail domain

in human P5CS may be superfluous for the purpose of proline and ornithine biosynthesis although the strong conservation of a protein motif observed within this domain (with complete conservation at H784), suggests an important unidentified role for this motif in eukaryotes. Interestingly, the observed phylogeny of this domain suggests that it has co-evolved with the localisation of P5CS to the mitochondrion.

Moonlighting roles are defined as the evolutionary adoption of an unrelated function by a metabolic enzyme, and are increasingly being identified.[33–35] Novel functions may have evolved from the utilisation of different surfaces on the protein not required in its enzymatic function, or subtle alterations in structure that permit new functions. Such roles could clarify the lack of a pathological mechanism to explain genotype–phenotype correlations for many Mendelian disorders.[35] Absence of an adequate mechanistic basis for the association between the identified mutation in *ALDH18A1* described here and the observed phenotype suggests the possibility that disruption of unappreciated moonlighting functions of P5CS may underlie this novel neurocutaneous syndrome.

Acknowledgements
We thank K Gibson and D Markie for assistance with analysis, T Merriman for access to his control cohort, M Black for statistical analysis of disease allele frequencies, D Carne for performing the amino acid hydrolysis and E Ledgerwood and A McNaughton for assistance with immunocytochemistry. This research was funded by an Otago University Research Grant, and a University of Otago Postgraduate Research Scholarship.

Conflict of interest
The authors state no conflict of interest.

References
1 Gupta N, Phadke SR: Cutis laxa type II and wrinkly skin syndrome: distinct phenotypes. *Pediatr Dermatol* 2006; **23**: 225–230.
2 Tassabehji M, Metcalfe K, Hurst J *et al*: An elastin gene mutation producing abnormal tropoelastin and abnormal elastic fibres in a patient with autosomal dominant cutis laxa. *Hum Mol Genet* 1998; **7**: 1021–1028.
3 Kaler SG, Gallo LK, Proud VK *et al*: Occipital horn syndrome and a mild Menkes phenotype associated with splice site mutations at the MNK locus. *Nat Genet* 1994; **8**: 195–202.
4 Hucthagowder V, Sausgruber N, Kim KH, Angle B, Marmorstein LY, Urban Z: Fibulin-4: a novel gene for an autosomal recessive cutis laxa syndrome. *Am J Hum Genet* 2006; **78**: 1075–1080.
5 Loeys B, Van Maldergem L, Mortier G *et al*: Homozygosity for a missense mutation in fibulin-5 (FBLN5) results in a severe form of cutis laxa. *Hum Mol Genet* 2002; **11**: 2113–2118.
6 Agha A, Sakati NO, Higginbottom MC, Jones Jr KL, Bay C, Nyhan WL: Two forms of cutis laxa presenting in the newborn period. *Acta Paediatr Scand* 1978; **67**: 775–780.
7 Morava E, Wopereis S, Coucke P *et al*: Defective protein glycosylation in patients with cutis laxa syndrome. *Eur J Hum Genet* 2005; **13**: 414–421.
8 Van Maldergem L, Yuksel-Apak M, Kayserili H *et al*: *The Debre type of autosomal recessive cutis laxa is associated with brain dysgenesis or neurodegeneration and defective N-glycosylation: The American Society of Human Genetics 57th Annual Meeting*. San Diego: American Society of Human Genetics, 2007.
9 Kornak U, Reynders E, Dimopoulou A *et al*: Impaired glycosylation and cutis laxa caused by mutations in the vesicular H+-ATPase subunit ATP6V0A2. *Nat Genet* 2008; **40**: 32–34.
10 Wu X, Steet RA, Bohorov O *et al*: Mutation of the COG complex subunit gene COG7 causes a lethal congenital disorder. *Nat Med* 2004; **10**: 518–523.
11 Al-Gazali LI, Sztriha L, Skaff F, Haas D: Gerodermia osteodysplastica and wrinkly skin syndrome: are they the same? *Am J Med Genet* 2001; **101**: 213–220.
12 Boente Mdel C, Asial RA, Winik BC: Geroderma osteodysplastica. Report of a new family. *Pediatr Dermatol* 2006; **23**: 467–472.
13 Boente MC, Winik BC, Asial RA: Wrinkly skin syndrome: ultrastructural alterations of the elastic fibers. *Pediatr Dermatol* 1999; **16**: 113–117.
14 Gorlin RJ, Cohen Jr MM: Craniofacial manifestations of Ehlers-Danlos syndromes, cutis laxa syndromes, and cutis laxa-like syndromes. *Birth Defects Orig Artic Ser* 1989; **25**: 39–71.
15 Steiner CE, Cintra ML, Marques-de-Faria AP: Cutis laxa with growth and developmental delay, wrinkly skin syndrome and geroderma osteodysplastica: a report of two unrelated patients and a literature review. *Gen Mol Biol* 2005; **28**: 181–190.
16 Zlotogora J: Wrinkly skin syndrome and the syndrome of cutis laxa with growth and developmental delay represent the same disorder. *Am J Med Genet* 1999; **85**: 194.
17 Gazit E, Goodman RM, Katznelson MB, Rotem Y: The Wrinkly Skin Syndrome: a new heritable disorder of connective tissue. *Clin Genet* 1973; **4**: 186–192.
18 Reisner SH, Seelenfreund M, Ben-Bassat M: Cutis laxa associated with severe intrauterine growth retardation and congenital dislocation of the hip. *Acta Paediatr Scand* 1971; **60**: 357–360.
19 de Barsy AM, Moens E, Dierckx L: Dwarfism, oligophrenia and degeneration of the elastic tissue in skin and cornea. A new syndrome? *Helv Paediatr Acta* 1968; **23**: 305–313.
20 Bartsocas CS, Dimitriou J, Kavadias A, Kyrzopoulos D: De Barsy syndrome. *Prog Clin Biol Res* 1982; **104**: 157–160.
21 Pontz BF, Zepp F, Stoss H: Biochemical, morphological and immunological findings in a patient with a cutis laxa-associated inborn disorder (De Barsy syndrome). *Eur J Pediatr* 1986; **145**: 428–434.
22 Baumgartner MR, Hu CA, Almashanu S *et al*: Hyperammonemia with reduced ornithine, citrulline, arginine and proline: a new inborn error caused by a mutation in the gene encoding delta(1)-pyrroline-5-carboxylate synthase. *Hum Mol Genet* 2000; **9**: 2853–2858.
23 Baumgartner MR, Rabier D, Nassogne MC *et al*: Delta1-pyrroline-5-carboxylate synthase deficiency: neurodegeneration, cataracts and connective tissue manifestations combined with hyperammonaemia and reduced ornithine, citrulline, arginine and proline. *Eur J Pediatr* 2005; **164**: 31–36.
24 Hu CA, Lin WW, Obie C, Valle D: Molecular enzymology of mammalian Delta1-pyrroline-5-carboxylate synthase. Alternative splice donor utilization generates isoforms with different sensitivity to ornithine inhibition. *J Biol Chem* 1999; **274**: 6754–6762.
25 Wakabayashi Y, Henslee JG, Jones ME: Pyrroline-5-carboxylate synthesis from glutamate by rat intestinal mucosa. Subcellular localization and temperature stability. *J Biol Chem* 1983; **258**: 3873–3882.
26 Kruglyak L, Daly MJ, Reeve-Daly MP, Lander ES: Parametric and nonparametric linkage analysis: a unified multipoint approach. *Am J Hum Genet* 1996; **58**: 1347–1363.
27 Markianos K, Daly MJ, Kruglyak L: Efficient multipoint linkage analysis through reduction of inheritance space. *Am J Hum Genet* 2001; **68**: 963–977.

28 Gyapay G, Morissette J, Vignal A *et al*: The 1993–94 Genethon human genetic linkage map. *Nat Genet* 1994; **7**: 246–339.
29 Husek P: Chloroformates in gas chromatography as general purpose derivatizing agents. *J Chromatogr B Biomed Sci Appl* 1998; **717**: 57–91.
30 Ng PC, Henikoff S: SIFT: predicting amino acid changes that affect protein function. *Nucleic Acids Res* 2003; **31**: 3812–3814.
31 Lander E, Kruglyak L: Genetic dissection of complex traits: guidelines for interpreting and reporting linkage results. *Nat Genet* 1995; **11**: 241–247.
32 Lander ES, Schork NJ: Genetic dissection of complex traits. *Science* 1994; **265**: 2037–2048.
33 Jeffery CJ: Moonlighting proteins. *Trends Biochem Sci* 1999; **24**: 8–11.
34 Jeffery CJ: Molecular mechanisms for multitasking: recent crystal structures of moonlighting proteins. *Curr Opin Struct Biol* 2004; **14**: 663–668.
35 Sriram G, Martinez JA, McCabe ER, Liao JC, Dipple KM: Single-gene disorders: what role could moonlighting enzymes play? *Am J Hum Genet* 2005; **76**: 911–924.